

## Inverse modeling of water retention curves in soils with different uses and coverings

*Modelagem inversa de curvas de retenção de água em solos com diferentes usos e coberturas*

Ana Flávia Cordeiro de Brito <sup>\*1</sup>(ORCID 0009-0004-0534-8433), Marcella Cardoso Teixeira <sup>1</sup>(ORCID 0009-0008-9061-313X), Lorene Alves de Oliveira <sup>1</sup>(ORCID 0009-0003-4763-3905), Adriana Magalhães Farias <sup>1</sup>(ORCID 0009-0002-6747-0560), Maria Ângela Cruz Macêdo dos Santos <sup>2</sup>(ORCID 0000-0003-1418-7438), Alisson Macendo Amaral <sup>1</sup>(ORCID 0000-0003-3035-2763)

<sup>1</sup>Federal Institute of Northern Minas Gerais, Arinos, MG, Brazil. \*Corresponding author: [alisson.amaral@ifnmg.edu.br](mailto:alisson.amaral@ifnmg.edu.br)

<sup>2</sup>Minas Gerais Institute of Agriculture and Livestock, Burity, MG, Brazil.

Submission: June 4, 2024 | Acceptance: July 22, 2024

### ABSTRACT

The soil water retention curve (CRAS) is an important hydraulic property for understanding soil water dynamics and relevant for efficient irrigation management. Inverse modeling has been widely accepted to determine CRAS due to its efficiency, especially on a large scale. The objective of this study was to determine and compare soil water retention curves through inverse modeling, in a red latosol, Cerrado phase, under different uses and soil covers. The accuracy of the curves was also evaluated using statistical indicators. For this, preserved and non-preserved samples were collected in the study areas in order to determine the structural characteristics of the soils, the physical-hydric properties and the humidity and evaporation curves, necessary to provide the Hydrus-1D model used in computational modeling. The statistical indicators coefficient of determination, mean error, root mean square error, Akaike Information Criterion and Bayesian Information Criterion demonstrated effectiveness in the modeled water retention curves. The areas of degraded Cerrado and conventional cultivation presented retention curves with higher water retention rates, compared to the organic cultivation area, result of structural changes in the systems, such as distribution and uniformity of pores. It was observed that a higher organic matter content associated with the sandy texture, in the organic cultivation area, resulted in lower water retention at low tensions (~ 348.50 kPa) sufficient to drain the water content in this system.

**KEYWORDS:** Hydrus 1D. Soil Properties. Hydraulic Flow.

### RESUMO

A curva de retenção de água no solo (CRAS) é uma propriedade hidráulica importante para entender a dinâmica da água no solo e relevante na gestão eficiente da irrigação. A modelagem inversa tem sido amplamente aceita para determinar a CRAS, devido a sua eficiência, especialmente em larga escala. O objetivo deste estudo foi determinar e comparar as curvas de retenção de água no solo por meio de modelagem inversa, em latossolo vermelho, fase cerrado, sob diferentes usos e coberturas de solos. Também foram avaliadas as acurácias das curvas por meio de indicadores estatísticos. Para isso, amostras preservadas e não preservadas foram coletadas nas áreas de estudo a fim de determinar as características estruturais dos solos, as propriedades físico-hídricas e as curvas de umidade e evaporação, necessárias para abastecer o modelo Hydrus-1D usado na modelagem computacional. Os indicadores estatísticos coeficiente de determinação, erro médio, raiz do erro quadrático médio, Critério de Informação de Akaike e o Critério de Informação Bayesiano demonstraram eficácia nas curvas de retenção de água modeladas. As áreas de cerrado degradado e cultivo convencional apresentaram curvas de retenção com taxas de retenção de água maiores, se comparadas com a área de cultivo orgânico, resultado das mudanças estruturais dos sistemas, como a distribuição e uniformidade de poros. Observou-se que maior teor de matéria orgânica associado à textura arenosa, na área de cultivo orgânico, resultou em menor retenção de água e que tensões baixas (~ 348,50 kPa) são suficientes para drenar o conteúdo de água nesse sistema.

**PALAVRAS-CHAVE:** Hydrus 1D. Propriedade do solo. Fluxo hidráulico.

## INTRODUCTION

Due to rapid population growth and decreasing water availability, irrigated agriculture causes significant negative impacts in many regions of the world, and any improvement in current irrigation practices can contribute to preserving limited water resources and promoting sustainable agriculture (HIMANSHU et al. 2021). Irrigated agriculture is dependent on the conditions of water absorption, movement, and distribution in the soil; therefore, its physical and hydrological properties are of significant interest.

Determining the hydraulic properties related to water dynamics in the soil, considering its intrinsic variations, is essential for defining irrigation parameters and adopting better water management strategies in crops (KET et al. 2018, HUANG et al. 2018, KUMAR et al. 2022).

The soil water retention curve (CRAS) represents the relationship between the soil matric potential ( $\Psi_m$ ) and the volumetric water content of the soil ( $\theta$ ), and is considered a fundamental property for understanding the hydraulic behavior of the soil and estimating the availability of water that can be used by plants (MORET-FERNANDEZ & LATORRE 2022).

One of the applications of this curve is irrigation management, which aims to raise water in the soil to desirable potentials, such as field capacity, for example, which is the maximum soil moisture without damaging the system (BERNARDO et al. 2006) and lower moisture levels at higher stresses, as is the case with desirable water deficits in fruit trees, such as in the case of mango cultivation to induce flowering (COELHO et al. 2002) and coffee, for induction and uniformity of flowering (MASARIRAMBI et al. 2009). Due to its importance, it is desirable that the soil water retention curve be determined accurately and efficiently.

Among the methods developed to determine the soil water retention curve, one of the most widely used is the tension table method. This method is classified as a direct and also costly method, both in terms of the need for specific infrastructure (laboratories, tension table, supplies) and in terms of the technical and scientific knowledge required to operate it. Therefore, due to these limitations, the indirect approach through computational modeling, such as the inverse model, has been widely used and accepted because it has a relatively simple configuration and processing, especially on a large scale, in addition to providing results with efficient estimates (KUMAR et al. 2022, LI et al. 2018).

Due to the Marquardt-Levenberg type optimization algorithm, the Hydrus-1D agro-hydrological model has become a useful tool for estimating soil hydraulic parameters from observed data through inverse modeling (SIMUNEK et al. 2013). This model numerically solves the Richards equation, which concerns the movement of water in the soil, and simulates this movement in a saturated/unsaturated porous medium. It is generally preferred due to its simplicity compared to parameterized physically-based models (ER-RAKI et al. 2021, SANTOS et al. 2018), such as Simple Soil Plant Atmosphere (SiSPAT) (BRAUD et al. 1995) and Interactions between Soil-Biosphere-Atmosphere (ISBA) (NOILHAN et al. 1996).

Estimating soil hydraulic properties through inverse modeling has been a research tool under different experimental conditions, such as those conducted by

SIMUNEK et al. 2013, GONZALEZ et al. 2015, NASCIMENTO et al. 2018 and SILVA et al. 2020a. These studies observed that the parameters obtained through inverse modeling have accuracy and representativeness in expressing the dynamics of water in the soil. Several factors can influence soil water dynamics, including soil characteristics such as texture, organic matter content, and porosity, as well as land use and land cover (JIA et al. 2017).

Considering the above, this study aims to determine and compare soil water retention curves through inverse modeling in a red latosol, cerrado phase, under different land uses and land covers.

## MATERIALS AND METHODS

### 2.1 Study area and soil analysis

The study was conducted on the premises of the Federal Institute of Northern Minas Gerais - Arinos Campus (Figure 1), whose soil is characterized as a Dystrophic Red Latosol.

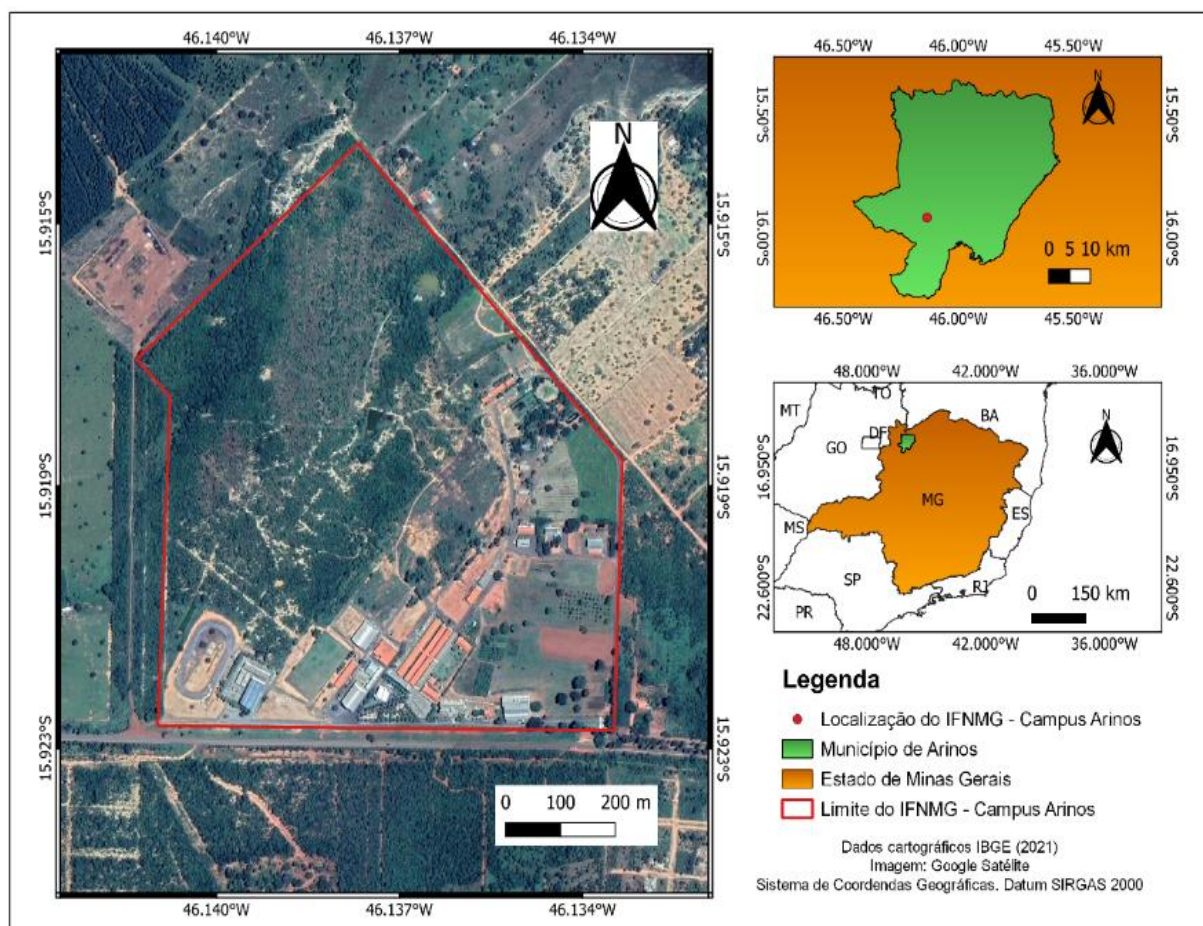


**Figure 1.** Experimental sample collection area.

Unpreserved and preserved soil samples were collected at a depth of 0-20 cm in three distinct areas: two anthropized areas, corresponding to conventional and organic production systems; and the third, a degraded Cerrado area (preservation area). Soil samples were collected with the objective of establishing physical and hydraulic properties of water in the soil, such as particle size distribution (sand, silt, clay) and soil density, which are hydraulic parameters required by the Hydrus-1D model.

In each study area, unpreserved samples were collected using a Dutch auger at representative points to form a composite sample. The samples were placed in plastic bags and properly labeled (depth and area). The preserved samples were collected using metallic volumetric cylinders with volumes of 83.81 cm<sup>3</sup> and 100.27 cm<sup>3</sup> (Kopeck cylinders), with three repetitions per area.

For the granulometric characterization of the soils (sand, silt, and clay), the non-preserved samples were sent to the Nativa agricultural analysis laboratory (Formosa-GO). The preserved samples were sent to the Soil Laboratory of the FINMG - Arinos Campus for determination of physical properties: bulk density (Bd), particle density (Pd), and total porosity (TP), according to the methodology of the Manual of Soil Analysis Methods (TEIXEIRA et al. 2017). For this purpose, the samples were dried in a forced-air oven at a temperature of 105-110 °C for a period of 48 hours. After drying, the overall density was calculated using Equation 1:

$$Bd = \frac{4 D_{ss}}{\pi d^2 h} \quad (1)$$

Where: Bd - Bulk soil density, in g/cm<sup>3</sup>; D<sub>ss</sub> - Dry mass of the soil, in grams; d - diameter of the volumetric ring, in cm; and h - height of the volumetric ring, in cm.

The particle density was determined by the volumetric flask method. Initially, 50 mL volumetric flasks were pre-calibrated with deionized and deaerated water, then 20 g of oven-dried soil at 105 °C were transferred using a funnel. The volume was completed by adding ethyl alcohol until the sample was covered, followed by shaking to remove bubbles and resting for 30 minutes. The sample volume was obtained by the difference between the volume of alcohol needed to fill the flask and the volume of liquid needed to complete the volume of the flask containing the dry sample. After this procedure, the particle density was determined by Equation 2.

$$p_d = \frac{m_a}{(V_T - V_u)} \quad (2)$$

Where: Pd - particle density, in g/cm<sup>3</sup>; m<sub>a</sub> - mass of the sample dried at 105 °C, in g; V<sub>T</sub> - total measured volume of the flask, in mL; and V<sub>u</sub> - volume used to fill the flask with the sample, in mL.

Total porosity was calculated using the indirect method, with Equation 3.

$$TP = \left(1 - \frac{Sd}{Pd}\right) 100 \quad (3)$$

Where: TP - total porosity, in %; Pd - soil particle density, in g cm<sup>-3</sup> and; Sd - soil density, in g cm<sup>-3</sup>.

## 2.2 Inverse modeling with Hydrus - 1D

In this stage, and in order to supply the Hydrus-1D version 4.17.0140 model (SIMUNEK et al. 2013), it is necessary to determine the volumetric water content curves and evaporation over time. To this end, a soil evaporation experiment was set up in triplicate in the laboratory, similar to the studies conducted by Silva et al. (2020b) and ŠIMUNEK et al. (1998). In this phase, soil blocks were recreated from unpreserved

samples from each area and from the previous determination of the bulk densities of each production system.

The unpreserved soil samples were air-dried, sieved, and packed according to their previously established densities into PVC (polyvinyl chloride) tubes with a diameter of 70 mm and a height of 150 mm. To prevent soil loss and allow free movement of water during the saturation phase, the bottom of each tube had a device made with shade cloth, according to procedures adopted by MENDES et al. (2021) and SANTOS et al. (2022 b).

In the laboratory, triplicate sets of "cylinder + soil" samples were saturated by capillarity over a period of 72 hours in order to eliminate any air fraction in the samples. After this procedure, the mass of the set was determined under saturated conditions. Then, the samples were subjected to gravitational drainage until they reached field capacity (at which point gravitational drainage ceased).

Subsequently, the samples were subjected to forced drying in an oven at temperatures of 30, 50, 70, 90, and 105 °C for a period of 12 days. Successive mass measurements were taken in order to construct the volumetric moisture content versus time curve. Mass variations were measured using a precision balance (0.001 g). The total amount of evaporated water in mm was determined by calculating the difference between the humidity values and relating them to the evaporation area of the tubes. The values of volumetric moisture content ( $\theta$ ,  $\text{cm}^3 \text{cm}^{-3}$ ) and evaporation (mm) are the input data for the Hydrus-1D model used in the simulations; therefore, the moisture content was established based on mass (gravimetric moisture content) -  $U$ ,  $\text{g g}^{-1}$ ) (Equation 4) and subsequently converted to a volume basis (volumetric moisture content) -  $\theta$ ,  $\text{cm}^3 \text{cm}^{-3}$ ) (Equation 5).

$$S = \frac{(Ms - Mds)}{Mds} \quad (4)$$

Where: S - Soil moisture ( $\text{g g}^{-1}$ ); Ms - mass of wet soil (g) and Mds - mass of dry soil (g).

$$\theta = S \frac{\rho}{\rho_a} \quad (5)$$

Where:  $\theta$  - volumetric moisture content ( $\text{cm}^3 \text{cm}^{-3}$ ); S - Soil moisture ( $\text{g g}^{-1}$ );  $\rho$  - bulk soil density ( $\text{g cm}^{-3}$ ) and  $\rho_a$  - density of water ( $\text{g cm}^{-3}$ ).

For the inverse modeling, the established boundary conditions were: upper boundary under atmospheric boundary conditions (evaporation data), zero flow at the lower boundary (zero drainage), and layer depth (15 cm - corresponding to the soil height in the tube) divided into nodes (intervals) of 1 cm (the program performs the simulation every 1 cm of the total soil volume).

The Hydrus-1D model has an associated Rosetta module (Neural Network Prediction) with which the soil's hydraulic parameters were established, based on data of bulk density ( $\text{g cm}^{-3}$ ) and particle size distribution (sand, silt, and clay in %). The hydraulic parameters obtained with the Rosetta module represent an initial hydraulic condition of the soils to begin the modeling.

In the simulations, the Mualem-Van Genuchten model (MUALEM 1976 & VAN

GENUCHTEN 1980) was used to establish the soil water retention curve (Equation 6) and the soil water conductivity curve (Equation 7).

$$\theta = \theta_{res} + (\theta_{sat} - \theta_{res})(1 + |\alpha h|^n)^{-m} \quad (6)$$

Where:  $\theta$  - soil moisture content ( $\text{cm}^3 \text{cm}^{-3}$ );  $\theta_{res}$  - residual soil moisture content ( $\text{cm}^3 \text{cm}^{-3}$ );  $\theta_{sat}$  - saturated soil moisture ( $\text{cm}^3 \text{cm}^{-3}$ );  $\alpha$ ,  $n$  and  $m$  - empirical factors, with  $m$  being dependent on  $n$  through the relationship (Equation 7):

$$m = 1 - \frac{1}{n} \quad (7)$$

According to the unsaturated hydraulic conductivity theory of VAN GENUCHTEN (1980), using the  $\theta(h)$  relationship, the  $K(\theta)$  function is defined as (Equation 8):

$$K = K_{sat} S_e^\lambda \left[ 1 - \left( 1 - S_e^m \right)^{m-2} \right] \quad (8)$$

Where:  $K_{sat}$  - is the saturated conductivity ( $\text{cm d}^{-1}$ );  $S_e$  - relative degree of saturation;  $\lambda$  - is a shape parameter (-) depending on the tortuosity of the flow path. And  $S_e$  defined as (Equation 9):

$$S_e = \frac{\theta - \theta_{res}}{\theta_{sat} - \theta_{res}} \quad (9)$$

The RICHARDS equation (1931) was used to estimate water flow in the soil (Equation 10).

$$\frac{\partial \theta}{\partial t} = \frac{\partial \left[ K(h) \left( \frac{\partial h}{\partial z} + 1 \right) \right]}{\partial z} - S(h) \quad (10)$$

Where:  $\theta$  - volumetric water content;  $t$  - is the time (d);  $K(h)$  - hydraulic conductivity ( $\text{cm d}^{-1}$ );  $h$  - water pressure potential in the soil (cm);  $z$  - vertical position calculated positively upwards (cm);  $S(h)$  - rate of water extraction from the soil by the roots ( $\text{m}^3 \text{m}^{-3} \text{d}^{-1}$ ).

The Hydrus-1D model, through spatio-temporal simulations, minimizes the differences between the obtained and simulated volumetric water content ( $\theta$ ) values in order to determine the soil hydraulic parameters ( $\alpha$ ,  $n$ ,  $\lambda$  and  $K_s$ ). The differences between the obtained and simulated  $\theta$  values are expressed through an objective function  $\Phi$  (Equation 11).

$$\phi(\theta, \beta) = \sum_{j=1}^m \sum_{i=1}^{n_j} [\theta_{OBT,j}(z_i, t_i) - \theta_{SML,j}(z_i, t_i, \beta)]^2 \quad (11)$$

Where:  $m$  - number of different measurement locations for  $\theta$ ;  $n$  - number of

measurements taken at each location  $m$ .

The equality represents the residual difference between the simulated water content values ( $\theta_{SML}$ ) using the optimized soil hydraulic parameters in  $\beta$  (that is,  $\theta_r$ ,  $\theta_s$ ,  $\alpha$ ,  $n$ ,  $K_s$  and  $\lambda$ ) and those obtained ( $\theta_{OBT}$ ) in time  $t_i$  for  $j$ -th measurements in  $z_i$ . The minimization of the objective function  $\Phi$  is performed using the Levenberg-Marquardt non-linear minimization method (SIMUNEK et al. 2013).

To evaluate the quality of the adjustments, the statistical indicators root mean square error (RMSE) (Equation 12), mean error (ME) (Equation 13), and coefficient of determination ( $R^2$ ) (Equation 14) were used as performance criteria, similar to GONZALEZ et al. 2015, REZAEI et al. 2016, WANG et al. 2016.

$$RMSE = \sqrt{\frac{1}{N} \sum_{t=1}^N (\theta_{obs} - \theta_{est})^2} \quad (12)$$

$$ME = \frac{1}{N} \sum_{t=1}^N (\theta_{obs} - \theta_{est}) \quad (13)$$

$$R^2 = \frac{SQR}{SQT} \quad (14)$$

Where: RMSE - root mean square error; ME - mean error; N - is the total number of observations;  $\theta_{obs}$  and  $\theta_{est}$  are the observed and simulated values for soil water content;  $R^2$  - coefficient of determination; SSR - sum of squares of the regression and SST - sum of squares total.

In addition to these, the Akaike information criterion (AIC) (Equation 15) and the Bayesian information criterion (BIC) (Equation 16) were adopted.

$$AIC = -2 \log \log L(\hat{\theta}) + 2k \quad (15)$$

$$BIC = -2 \log \log L(\hat{\theta}) + k \log \log n \quad (16)$$

Where:  $L(\hat{\theta})$  is the maximum likelihood function;  $k$  is the number of free parameters in the model;  $n$  is the number of observations in the sample. The term  $2k$  is the penalty term and acts as a compensation for the bias in the lack of fit when maximum likelihood estimators are used.

## RESULTS AND DISCUSSION



The granulometric characterization and physical properties of the soil for the study areas are presented in Table 1. The texture class was established using the Textural Triangle, according to SANTOS et al. (2005) and PHOGAT et al. (2016).

**Table 1.** Granulometric characterization and physical properties of soil samples for the study areas.

Area	Sand	Silt	Clay	Textural class	Bd	Pd	TP
	g kg <sup>-1</sup>	g kg <sup>-1</sup>	g kg <sup>-1</sup>		g cm <sup>-3</sup>	g cm <sup>-3</sup>	%
DC	440	240	320	Loamy-clay	1.44	2.02	28.67
CC	404	215	381	Clay	1.43	2.16	33.78
OC	455	142	403	Sandy-clay	1.45	2.38	39.01

DC: Degraded Cerrado; CC: Conventional cultivation; OC: Organic cultivation; Bd: Bulk density; Pd: Particle density; TP: Total porosity.

Table 2 presents the hydraulic parameters for each study area and the statistical indicators: coefficient of determination ( $R^2$ ), mean error (ME), root mean square error (RMSE), Akaike Information Criterion (AIC), and Bayesian Information Criterion (BIC), which express the quality of the fits achieved when comparing the measured and simulated soil water content. Statistical indicators are mathematical parameters used to evaluate the accuracy and precision of model predictions and help understand how well the model is describing the behavior of the system under study (PHOGAT et al. 2016).

**Table 2.** Soil hydraulic properties and statistical indicators for the study areas.

Area	$\theta_r$	$\theta_s$	$\alpha$	n	Ks	$\lambda$	RMSE	EM	$R^2$	AIC	BIC
	cm <sup>3</sup> cm <sup>-3</sup>	cm <sup>3</sup> cm <sup>-3</sup>	-	-	cm h <sup>-1</sup>	-	cm <sup>3</sup> cm <sup>-3</sup>	cm <sup>3</sup> cm <sup>-3</sup>	-	-	-
DC	0.078	0.429	0.016	1.373	0.465	0.5	0.077	0.026	0.85	-0.206	-0.198
CC	0.097	0.458	0.024	1.222	0.657	0.5	0.084	0.017	0.82	-0.189	-0.181
OC	0.086	0.440	0.021	1.283	0.617	0.5	0.083	0.015	0.84	-0.199	-0.191

DC: Degraded Cerrado; CC: Conventional cultivation; OC: Organic cultivation;  $\theta_r$ : wastewater content;  $\theta_s$ : saturated water content;  $\alpha$ , n,  $\lambda$ : empirical adjustment parameters; Ks: saturated hydraulic conductivity; RMSE: root mean square error EM: mean error;  $R^2$ : coefficient of determination; AIC: Akaike Information Criterion; BIC: Bayesian Information Criterion.

The  $R^2$  values found are similar to those reported by ER-RAKI et al. (2021) and AIRES et al. (2022), who also observed similar RMSE values in experiments conducted using the Hydrus model. In a previous study, the authors Mohammed et al. (2021) observed good agreement between the predicted and measured values for the hydraulic properties of the soil, with  $R^2$  values ranging from 0.78 to 0.99 and RMSE values ranging from 0.000012 to 0.146. For this study, it is observed that the  $R^2$  and RMSE values are within the range cited in the literature, which demonstrates the reliability of the model adjustments shown here.

The Degraded Cerrado area and the Conventional Cultivation area showed characteristic curves with a higher water retention rate, compared to the organic cultivation area, where low tensions are required to remove all the water content from the soil (Figure 2). According to the modeling, the tension at which the volumetric water content in the soil in Organic Farming is zero is equivalent to 368.50 kPa, that is, a low tension compared to the other systems (conventional and degraded).



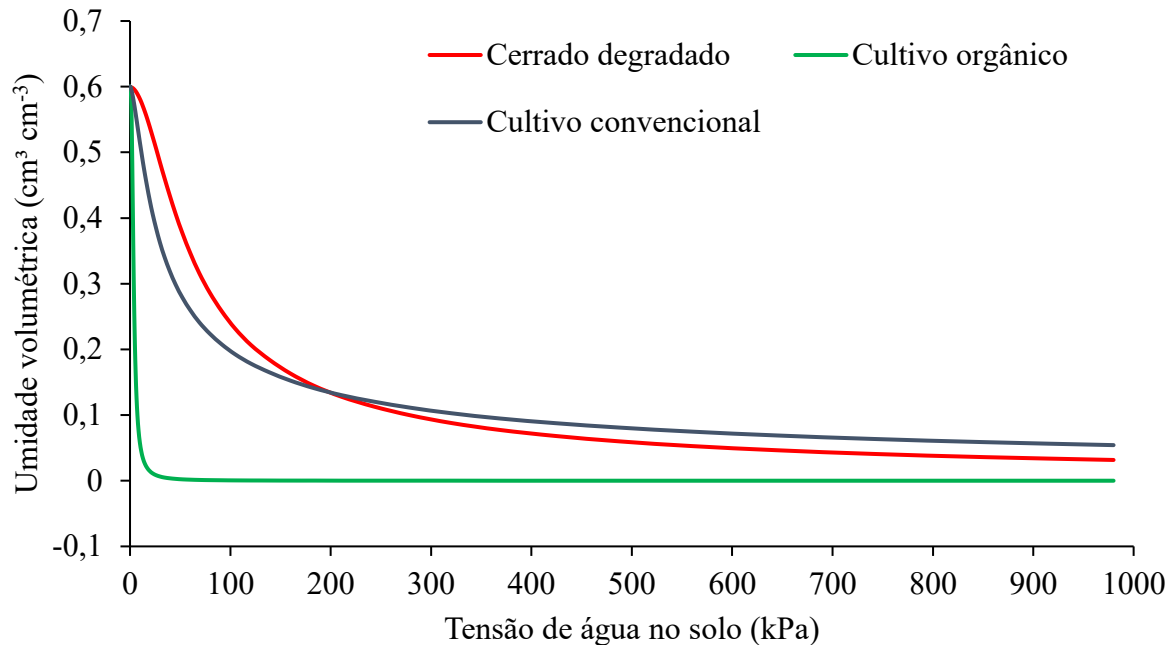


**Figure 2.** Soil water retention curves modeled for the degraded cerrado area (A), conventional cultivation (B), and organic cultivation (C), at a depth of 0-20 cm.

The water retention curve depends on the intrinsic characteristics of each soil, being influenced by the interaction of factors such as texture (EASTON & BOCK 2016), porosity, land use (DLAPA et al. 2020), and organic matter (LAL et al. 2020). It can be inferred that the organically cultivated area, even retaining a large initial volume of water due to a greater number of pores (Table 1), retains water at low tensions, being easily evaporated (Figure 2), since larger pores, when filled with water, are emptied more easily at potentials close to zero (SANTOS et al. 2022a) due to a higher inherent hydraulic conductivity at higher moisture levels.

Changes in porosity cause modifications in the behavior of the soil water retention curve, where experimental tests on sandy-clay soil with different porosities show that suction varies significantly with changes in porosity, decreasing as porosity increases. Consequently, the reduction in the volumetric water content in the soil becomes faster (LIU et al. 2020).

The higher porosity in the organic farming area (Table 1), compared to the other areas, can be attributed to the type of land use and the amount of organic matter present, as it is an area characterized by organic agriculture and the adoption of conservation farming practices. Areas with high organic matter content positively influence the improvement of basic soil hydraulic properties, including particle size distribution, bulk density, porosity, and water retention capacity (DLAPA et al. 2020). In this sense, there are reductions in soil bulk density and tensile strength, an increase in porosity, an increase in the proportion of soil aggregation, mainly those stable in water, an improvement in the infiltration rate, and an increase in saturated hydraulic conductivity (CANQUI 2017, KLEIN & KLEIN 2015). However, these authors state that in soils with a more sandy texture, retention is more sensitive to the amount of organic matter than when compared to more clayey soils, which have a finer texture.

Regarding texture, high levels of sand can be observed in the organic farming area (Table 1), which also contributes to lower water retention in the soil. A lower water content was observed in horizons with a predominance of the sand fraction, in a study conducted by SILVA et al. (2020 a). In clay soils, such as those used in conventional cultivation (Table 1), the pores are more evenly distributed, which means that as the tension increases, the decrease in water content is more gradual (Figure 2).

Several studies have observed differences in water retention between soil types, profile depths, and particle size distributions, highlighting that soils with a finer texture and higher clay content, such as latosols, have a higher water retention capacity compared to soils with a coarser and sandier texture (KIEHL 1979, BRADY 1989, NÓBREGA et al. 2022), which explains the behavior observed in the water retention curve for the conventional cultivation area (Figure 2). Similar behavior is observed for the degraded cerrado area, but with a smaller volume of retained water, possibly due to changes in soil texture that interfere with water movement/flow (Table 1).

Clay soils may exhibit higher total porosity due to the greater microporosity provided by the higher clay content, resulting in greater water retention (MIOTTI et al. 2013). According to REICHARDT (1987), soils with a clayey texture have a greater distribution and uniformity of micropores, favoring the absorption of a larger amount of water and a gradual decrease in soil moisture. Besides, due to its high specific surface area and negative charge, the clay fraction adsorbs a large amount of water molecules to the soil surface, contributing to a greater volume of water retained in soils with a higher clay content (SILVA et al. 2018).

## CONCLUSION

The statistical indicators, including the coefficient of determination, mean error, root mean square error, Akaike Information Criterion, and Bayesian Information Criterion, demonstrated effectiveness in the modeled water retention curves.

Porosity, texture, and the presence of organic matter play a crucial role in the dynamics of water in the soil, influencing the water retention curve.

The organic cultivation area showed a soil water retention curve with a lower retention rate due to greater porosity, possibly because of a higher amount of organic matter present.

The greater distribution and uniformity of pores in the conventional and degraded cerrado cultivation areas were responsible for greater water retention at higher tensions.

## AUTHOR'S CONTRIBUTIONS

Conceptualization, methodology, and formal analysis, BRITO, A. F. C, SANTOS, M. Â. C.M and AMARAL, A. M.; validation, SANTOS, M. Â. C. M and AMARAL, A. M.; investigation, BRITO, A. F. C, TEIXEIRA, M. C., OLIVEIRA, L. A. and FARIAS, A. M.; data curation, SANTOS, M. Â. C. M and AMARAL, A. M.; writing - original draft preparation, BRITO, A. F. C; writing - review and editing, BRITO, A. F. C, SANTOS, M. Â. C. M and AMARAL, A. M.; supervision, SANTOS, M. Â. C. M and AMARAL, A. M.; project administration, AMARAL, A. M.; funding acquisition, AMARAL, A. M. All authors have read and agreed to the published version of the manuscript.

## FINANCING

This work was developed with the support of scientific initiation scholarships granted by the National Council for Scientific and Technological Development (CNPq) and the Federal Institute of Northern Minas Gerais (IFNMG). There was no financial support through specific funding programs; however, the project activities were made possible with institutional resources provided by the originating institution (IFNMG).

## DATA AVAILABILITY STATEMENT

The data can be made available upon request.

## ACKNOWLEDGEMENTS

The authors express their gratitude to the National Council for Scientific and Technological Development (CNPq) and the Federal Institute of Northern Minas Gerais (IFNMG), which provided scientific initiation scholarships and the necessary infrastructure for conducting the research.

## CONFLICTS OF INTEREST

The authors declare that they have no conflicts of interest related to this research.

## REFERENCES

- AIRES et al. 2022. Umidade do solo e estresse hídrico simulado com Hydrus-1D em área com sorgo forrageiro irrigado. *Agrometeoros* 30: 1-7.
- BERNARDO et al. 2006. Manual de Irrigação. 8.ed. Viçosa: Editora UFV.
- BRADY NC. 1989. Natureza e propriedade dos solos. 7.ed. Rio de Janeiro: Freitas Bastos.
- BRAUD et al. 1995. A simple soil-plant-atmosphere transfer model (SiSPAT) development and field verification. *Journal of Hydrology* 166: 213-250.
- CANQUI HB. 2017. Biochar and soil physical properties. *Soil Science Society of America Journal* 81: 687-711.
- COELHO et al. 2002. A cultura da mangueira. Brasília: Embrapa. p. 167-189.
- DLAPA et al. 2020. The impact of land-use on the hierarchical pore size distribution and water retention properties in Loamy soils. *Water* 339: 1-13.
- EASTON ZM & BOCK E. 2016. Soil and Soil Water Relationships. Virginia: Virginia Cooperative Extension. Disponível em: [https://ext.vt.edu/content/dam/ext\\_vt\\_edu/topics/agriculture/water/documents/Soil-and-Soil-Water-Relationships.pdf](https://ext.vt.edu/content/dam/ext_vt_edu/topics/agriculture/water/documents/Soil-and-Soil-Water-Relationships.pdf). Acesso em: 15/04/2024 às 16:30 hs.
- ER-RAKI et al. 2021. Performance of the HYDRUS-1D model for water balance components assessment of irrigated winter wheat under different water managements in semi-arid region of Morocco. *Agricultural Water Management* 244: 1-13.
- GONZALEZ et al. 2015. Modelling soil water dynamics of full and deficit drip irrigated maize cultivated under a rain shelter. *Biosystems Engineering* 132: 1-18.

- HIMANSHU et al. 2021. Simulated efficient growth-stage-based deficit irrigation strategies for maximizing cotton yield, crop water productivity and net returns. *Agricultural Water Management* 250: 1-12.
- HUANG et al. 2018. Soil water extraction monitored per plot across a field experiment using repeated electromagnetic induction surveys. *Soil Systems* 11: 1-17.
- JIA et al. 2017. Soil moisture decline due to afforestation across the Loess Plateau, China. *Journal of Hydrology* 546: 113-22.
- KET et al. 2018. Estimating soil water retention curve by inverse modelling from combination of in situ dynamic soil water content and soil potential data. *Soil Systems* 55: 1-23.
- KIEHL ED. 1979. Manual de edafologia: relações solo-planta. São Paulo: Editora Agronômica Ceres.
- KLEIN C & KLEIN VA. 2015. Estratégias para potencializar a retenção e disponibilidade de água no solo. *REGET* 19: 21-29.
- KUMAR et al. 2022. Site-specific irrigation scheduling using one-layer soil hydraulic properties and inverse modeling. *Agricultural Water Management* 273: 2-13.
- LAL R. 2020. Soil organic matter and water retention. *Agronomy Journal* 112: 3265-3277.
- LI et al. 2018. Inverse modeling of soil hydraulic parameters based on a hybrid of vector-evaluated genetic algorithm and particle swarm optimization. *Water* 10: 1-23.
- LIU et al. 2020. Effect of porosity on soil-water retention curves: Theoretical and experimental aspects. *Geofluids Special edition*: 1-8.
- MASARIRAMBI et al. 2009. The effect of irrigation on synchronization of coffee (*Coffea arabica* L.) flowering and berry ripening at Chipinge, Zimbabwe. *Physics and Chemistry of the Earth* 34: 786-789.
- MENDES et al. 2021. Calibração de sonda de baixo custo para monitorar umidade em substrato comercial. *Meio Ambiente Brasil (MABRA)* 3: 89-95.
- MIOTTI et al. 2013. Profundidade e atributos físicos do solo e seus impactos nas raízes de bananeiras. *Revista Brasileira de Fruticultura* 35: 536-545.
- MOHAMMED et al. 2021. Using inverse modeling by Hydrus-1D to predict some soil hydraulic parameters from soil water evaporation. *Colombia Forestal* 25: 21-35.
- MORET-FERNANDEZ & LATORRE. 2022. A novel double disc method to determine soil hydraulic properties from drainage experiments with tension gradients. *Journal of Hydrology* 615: 1-14.
- MUALEM Y. 1976. A new model for predicting the hydraulic conductivity of unsaturated porous media. *Water Resources Research* 12: 513-522.
- NASCIMENTO et al. 2018. Estimation of van Genuchten equation parameters in laboratory and through inverse modeling with Hydrus-1D. *Journal of Agricultural Science* 10: 102-110.
- NÓBREGA et al. 2022. Funções de pedotransferência para estimar a retenção e a disponibilidade de água em Planossolo Háptico sob sistemas integrados de produção agropecuária no Agreste da Paraíba. *Scientia Plena* 8: 1-19.
- NOILHAN et al. 1996. The ISBA land surface parametrisation scheme. *Global and Planetary Change* 13: 145-159.

- PHOGAT et al. 2016. Statistical Assessment of a numerical model simulating agro hydrochemical processes in soil under drip fertigated mandarin tree. *Irrigation and Drainage Systems Engineering* 5: 1-9.
- REICHARDT K. 1987. *A água em sistemas agrícolas*. São Paulo: Manole.
- REZAEI et al. 2016. The relevance of in-situ and laboratory characterization of sandy soil hydraulic properties for soil water simulations. *Journal of Hydrology* 534: 251-265.
- RICHARDS LA. 1931. Capillary conduction of liquids through porous mediums. *Physics* 1: 318-333.
- SANTOS et al. 2022a. Water retention and availability in tropical soils of different textures amended with biochar. *Catena* 219: 1-8.
- SANTOS et al. 2022b. Evaluation of low-cost electronic sensors for monitoring soil moisture in an experimental area in the brazilian semiarid. *Sensor Review* 42: 648-656.
- SANTOS et al. 2005. *Manual de descrição e coleta de solos no campo*. 5.ed. Viçosa: Sociedade Brasileira de Ciência de Solo (SBCS).
- SANTOS et al. 2018. Conteúdo volumétrico da água no solo via modelos de competição interespecífica. *Pesquisa e Ensino em Ciências Exatas e da Natureza* 2 (ed. especial): 30-39.
- SILVA et al. 2018. Soil water retention curve as affected by sample height. *Revista Brasileira de Ciência do Solo* 42: 1-13.
- SILVA et al. 2020a. Caracterização físico-hídrica de solos arenosos através da curva de retenção de água, índice S e distribuição de poros por tamanho. *Agrarian* 13: 478-492.
- SILVA et al. 2020b. Determination of soil hydraulic properties and its implications for mechanistic simulations and irrigation management. *Irrigation Science* 38: 223-234.
- SIMUNEK et al. 2013. *The HYDRUS-1D Software Package for Simulating the One-Dimensional Movement of Water, Heat, and Multiple Solutes in Variably-Saturated Media*. California: Riverside.
- ŠIMŮNEK et al. 1998. *The hydrus-1d software package for simulating the one-dimensional movement of water, heat, and multiple solutes in variably saturated media: Tutorial*. Australia: CSIRO Land and Water.
- TEIXEIRA et al. 2017. *Manual de métodos de análise de solo*. 3.ed. Brasília: Editora Embrapa.
- VAN GENUCHTEN MT. 1980. A closed-form equation for predicting the hydraulic conductivity of unsaturated soils. *Soil Science Society of America Journal* 44: 892-898.
- WANG et al. 2016. Feasibility analysis of using inverse modeling for estimating natural groundwater recharge from a large-scale soil moisture monitoring network. *Journal of Hydrology* 533: 250-265.